Palm Oil Biomass Supply Chain Multi-Objective Two-Echelon Location-Routing Optimization

Foo, F. Y.[1,2], Zainuddin, Z. M.[*1,3], and Hang, S. P.[1]

[1]*Department of Mathematical Sciences, Faculty of Science,*
Universiti Teknologi Malaysia, 81310 Johor Bahru, Johor
[2]*Mathematical Sciences Studies, College of Computing, Informatics and Mathematics,*
Universiti Teknologi MARA Johor Branch, Pasir Gudang Campus,
Jalan Purnama, Bandar Seri Alam, 81750 Masai, Johor
[3]*UTM Centre for Industrial and Applied Mathematics (UTM-CIAM),*
Ibnu Sina Institute for Scientific and Industrial Research (ISI-SIR),
Universiti Teknologi Malaysia, 81310 Johor Bahru, Johor, Malaysia

E-mail: zmarlizawati@utm.my
*Corresponding author

Abstract

Malaysia generates substantial agricultural residues annually, endowing the country with significant biomass energy potential. Palm oil biomass stands out as a promising feedstock. However, its high humidity, bulkiness, low energy density, and dispersed resource locations (mills) pose challenges. A network that consisting collection facilities incorporating pretreatment operations as intermediaries between mills and biorefineries is a plausible solution. Nevertheless, the facility locations directly impact travel distance, overall expenses, and the nearby population. Moreover, vehicle routing during biomass collection influences transportation costs and carbon dioxide (CO_2) emissions. Consequently, this research designs a model to address the location-routing intricacies within a two-echelon biomass supply chain. The model operates as a multi-objective optimization framework, encompassing three-dimensional sustainability assessment, quantified respectively as total cost minimization, CO_2 emissions reduction, and minimization of the population affected. The research initially optimizes each objective function individually and subsequently advances to multi-objective optimization employing the weighted sum approach. While single-objective optimization yields optimal outcomes for each dimension, enhancements in one aspect may hinder performance in others. Nonetheless, the multi-objective optimization provides insight into the trade-offs among the sustainability objectives. The computational findings demonstrate the model could adapt the network configuration in alignment with distinct sustainability aspirations.

Keywords: biomass supply chain; location-routing problem; mixed integer nonlinear programming; palm oil biomass; two-echelon location-routing model.

1   Introduction

As a major palm oil producer, Malaysia generates substantial quantities of palm oil empty fruit bunches (EFB) biomass, offering a promising source of biomass energy. Increasing biomass energy production will enhance the clean energy composition in Malaysia's overall energy generation, supporting Malaysia's pledge for sustainable development. However, there are numerous logistical and operational challenges to maximizing the benefits of biomass energy. The EFB resource sites that spread across rural and semi-urban regions might pose collection difficulties. The low energy density, high humidity, and bulky nature of biomass also lead to storage space issues, transportation difficulties, and reduced combustion efficiency. Hence, an efficient Biomass Supply Chain (BSC) is crucial. The architecture of the supply chain network is crucial to driving the profitability and productivity of the supply chain [28]. The motivation of this study is to address the challenges by optimizing the BSC network and supporting Malaysia's clean energy and sustainability commitments.

The BSC could be categorized into upstream, midstream, and downstream segments. The upstream includes biomass resources, pretreatment facilities, and storage centers [3, 20]. The midstream involves biorefineries and mixing plants [20], while the downstream covers biofuel storage and distribution to consumers [22]. The upstream segment is particularly interesting to examine, as it differs significantly from the middle and downstream segments, which resemble petroleum industry processes [3]. This study focuses on optimizing the BSC network, particularly the upstream and midstream segments, by delving into a network consisting of collection facilities with pretreatment operations. These collection centers can alleviate the challenge posed by dispersed resource sites. Pretreatment, such as pelletizing, reduces humidity and compresses biomass, thereby increasing its energy density [25]. Improved physical characteristics and energy density enhance storage, transportation, and combustion efficiency. The investigated BSC network involves palm oil mills (feedstock sources), collection facilities (intermediaries), and biorefineries (energy conversion).

The locations of collection facilities significantly affect the biomass supply chain by influencing travel distances and overall costs. Properly positioned facilities reduce operational costs by reducing the need for extra storage and lowering environmental impact through shorter transportation routes. In supply chain design, vehicle route planning is another major concern [27]. Poorly planned routes not only increase operational costs but also contribute to air pollution [31]. Efficient routes cut down transportation time and costs, improve resource utilization, and reduce CO_2 emissions. Operation Research (OR) principles address these challenges as Facility Location Problems (FLP) and Vehicle Routing Problems (VRP), respectively. While these problems are interconnected and contribute to the effectiveness of the BSC network, they are often tackled separately, potentially leading to suboptimal solutions [5]. Hence, this research aims to solve FLP and VRP simultaneously as a location-routing problem (LRP).

Generally, the objective of the BSC model is to establish an efficient framework that meets customer demand while minimizing costs. However, decisions within the BSC also impact the environment and society. Collection facilities might generate noise and release chemicals, making them unsuitable for placement in densely populated areas. Therefore, the BSC model should prioritize the least population areas for facility establishment to minimize the concentration of negative social impacts on communities (social performance). Furthermore, the substantial contribution of transportation-related CO_2 emissions to global warming should not be overlooked. Hence, the network design should incorporate route planning that minimizes total CO_2 emissions (environmental performance).

In this study, the logistical and operational challenges associated with the usage of EFB as biomass energy in BSC Malaysia is examined. The characteristics of biomass, including bulkiness, high humidity, and low energy density, combined with its distributed resource sites cause problems for collection, storage, transportation, and combustion efficiency. A BSC consisting of collection facilities equipped with pretreatment operations might be a plausible solution. Then, the associated collection facility placement and truck routing problems impact the overall performance of BSC. Suboptimal solutions may arise from handling these two core BSC research problems individually. Hence, this study aims to develop an LRP model that simultaneously optimizes the location of collection facilities and transportation routes to enhance the BSC's economic, environmental, and social performance.

A mixed-integer nonlinear programming model is introduced to address the LRP within a two-echelon BSC network comprising pretreatment operations. The model optimizes the collection facility locational and truck routing decisions while considering sustainability through cost minimization (economic performance), total CO_2 minimization (environmental performance), and total affected population minimization (social performance). In summary, this research establishes a distinct multi-objective two-echelon LRP (MO2ELRP) model for a palm oil EFB BSC network and quantifies the pretreatment operations into the model, setting it apart from a general two-echelon LRP (2ELRP) model.

This study proposes a novel approach in the context of BSC network optimization to optimize facility locations and truck routing decisions simultaneously. Additionally, the model offers a fundamental structure for managing the BSC network with one or various sustainability objectives, an aspect that has been less explored in previous LRP research within BSC contexts. Thirdly, the suggested model uniquely quantifies the pretreatment operations which makes it a distinction from the general LRP model. Finally, the model may be used to optimize any other BSC networks of various facilities utilizing diverse technologies.

This research has contributed to the BSC and LRP research in the following ways. The developed two-echelon network model including pretreatment operations enhances the practical applicability and effectiveness of model optimization in solving LRP in the context of BSC. By taking into consideration economic, environmental, and social performances, the model offers a framework for managing sustainable BSC. Since the model optimizes the locational and routing decisions simultaneously, it improves the overall BSC performance. Lastly, considering the modifications in biomass properties brought about by the pretreatment operation, the model has been adapted to the process in BSC and makes it different from the general LRP model.

The originality of the research lies in the holistic and versatility of the model. The integration of economic, environmental, and social performance goals into the LRP optimization model in the BSC context represents a holistic sustainable advancement in BSC investigation areas. The model could be applied to various BSC networks employing different technologies demonstrating its versatile utility and innovation. Further, this research has a foundational impact on future BSC research to incorporate multiple sustainability objectives and pretreatment operations into solving the LRP in the BSC.

The paper is structured into six sections: Section 2 provides an overview of optimization models in the BSC field, Section 3 defines the problem and assumptions, Section 4 presents the mathematical model, Section 5 outlines the results of computational experiments, and the final section presents conclusions and limitations.

2   Literature Review

In recent years, there has been a substantial body of research exploring the design of the Biomass Supply Chain (BSC) network. Most BSC studies have focused on various aspects of decision-making, such as resource allocation, facility location, and vehicle routing. Among these decisions, determining optimal facility locations holds paramount importance in shaping the network's structure. To address this challenge, Zhao and Li [58] employed binary integer programming to pinpoint the suitable location for a power plant, while Salleh et al. [38] utilized a least-squares regression approach for locating a biomass processing facility. Some researchers have addressed Facility Location Problems (FLP) while assessing crop availability by combining multi-criteria analysis with Geographic Information System (GIS) techniques, such as assessing the availability of corn stover and wheat straw [37], estimating forest residue supply [53], and evaluating manure availability from farms and wood density [17].

Research articles focused solely on the allocation problem have been documented as follows. While taking into account the limitation of vehicle capacity, the model of How and Lam [13] solved the biomass allocation problem. Wang et al. [52] formulated a model to estimate biomass supply and determine co-firing ratios for retrofit power plants. She et al. [44] explored wood residue salvaging in both sequential and integrated scenarios. Rivera-Cadavid et al. [33] created a model to decide which sugarcane biomass plots should be collected daily. Tiammee and Likasiri [48] addressed distribution and disposal issues related to corn residue.

The modeling of the location-allocation problem has also garnered substantial attention from researchers. Serrano-Hernandez and Faulin [43] developed a model to ascertain storage policies and determine biorefinery capacities and numbers. Saadati and Hosseininezhad [35] devised a network design for the bioethanol supply chain, taking into account road and railway transport. Sarker et al. [40, 41] addressed BSC issues involving resource sites, hubs, and reactors. Several studies have incorporated GIS into their research. Zhang et al. [56] combined GIS with simulation and optimization, while Zhang et al. [57] integrated GIS with optimization. Soha et al. [46] applied GIS and logistics analysis to optimize biogas supply chains. Other combinations of techniques found in the literature include combining GIS with nonlinear programming and evolutionary strategies [42], using GIS with the p-median model [15], integrating GIS with mixed-integer programming [36], and coupling GIS with robust optimization [32].

The challenges posed by vehicle routing and scheduling have captured significant attention due to their considerable contribution to overall expenses. In this arena, Torjai and Kruzslicz [50] established a model for biomass delivery schedules, while Soares et al. [45] synchronized truck pickup and delivery operations. Vahdanjoo et al. [51] utilized a vehicle routing model to solve the bale collection problem. Pinho et al. [30] proposed a predictive vehicle routing control model. Fokkema et al. [10] tackled a biogas logistic problem using a continuous-time inventory-routing model. Cárdenas-Barrón and Melo [6] examined the reverse logistics of waste vegetable oil collection, modeling it as a selective and periodic inventory-routing problem. Malladi et al. [23] investigated transshipment and routing plans for the forest supply chain, while Zamar et al. [55] designed routes for sawmill residue collection, considering biomass availability and humidity.

Researchers have started to delve into Location-Routing Problems (LRP), recognizing the inherent connection between FLP and Vehicle Routing Problems (VRP) (Table 1). In this context, Cao et al. [5] proposed solving FLP and VRP for the BSC concurrently. Morales Chavez et al. [7] developed a stochastic location-inventory-routing model for BSC. Habibi et al. [12] aimed to minimize costs in the location-inventory-routing model for the microalgae biofuel network. Working within a similar network, Asadi et al. [2] optimized economic and environmental performance.

A few studies have explored the LRP involving two echelons, exemplified by Li et al. [21] and Cao et al. [4]. However, Li et al. [21] focused on a network comprising a single end-user (power plant), while the design by Cao et al. [4] involved multiple customers (biorefineries).

In contrast, only a handful of articles have considered incorporating pretreatment operations into the network structure. San Juan et al. [39] developed a model that integrates feedstock quality and pretreatment operations. De Meyer et al. [9] quantified the pretreatment operations and biomass loss within their BSC model. Arabi et al. [1] formulated a network design considering pretreatment and deterioration rates in an algae-based supply chain.

Unsurprisingly, economic performance has been the central focus of the articles discussed thus far, given its pivotal role in BSC management. Nonetheless, environmental and social objectives can potentially conflict with economic goals. Few studies have addressed both economic and environmental performance in BSC. From the literature, minimizing total cost is often paired with minimizing CO_2 emissions, with studies focusing on emissions from transportation only [35, 58], transportation and combustion [39], or transportation and distribution facilities [2]. Other performance metrics in the literature include maximizing net revenues and greenhouse gas savings [44], maximizing profit and carbon absorption [1], and maximizing profit along with environmental sustainability satisfaction[13]. Moreover, the social sustainability aspects of BSC have been overlooked in most existing research. Few articles, such as those by Tiammee and Likasiri [48] and Morales Chavez et al. [7], have taken a broader view by designing network structures that account for all three dimensions, including the social dimension. Among the most common economic objectives is the minimization of total costs across the network. Similarly, the maximization of job creation is a prevalent social performance goal, and the assessment of total CO_2 emissions holds a significant influence in evaluating environmental performance.

Most articles addressing LRP in BSC have primarily targeted optimizing economic performance in Table 1. However, only a limited number of LRP articles have holistically considered all three dimensions. For instance, Asadi et al. [2] worked on economic and environmental performance, aiming to minimize total cost and system pollution. The LRP study encompassing sustainability from all dimensions is the work by Morales Chavez et al. [7], who designed a model to maximize net present value, minimize environmental impact, and maximize positive effects like job creation and food security.

An analysis of the existing literature reveals several gaps:

a) Few studies have tackled the solution of LRP within BSC, and fewer still have ventured into the realm of 2ELRP.

b) Research articles addressing the sustainability of solving LRP in BSC are lacking.

c) Existing LRP research in BSC rarely includes goals of minimizing CO_2 emissions and reducing the affected population.

d) Only a minority of research articles have incorporated pretreatment operations into their network models.

Table 1: Articles related to location-routing problems in the biomass supply chain.

Reference	LD	AD	RSD	PO	Eco	Env	Soc	Obj
[4]	●	●	●		●			Min total cost
[5]	●	●	●		●			Min total cost
[21]	●	●	●		●			Min total cost
[12]	●	●	●		●			Min total cost
[2]	●	●	●		●	●	●	Min total cost,
								Min total system pollution
[7]	●	●	●		●	●	●	Max net present value,
								Min environmental impact,
								Max positive impact
								(job creation and food security)

Note: LD = Locational Decision, AD = Allocation Decision, RSD = Routing or Scheduling Decision,
PO = Pretreatment Operation, Eco = Economic Performance, Env = Environmental Performance,
Soc = Social Performance, Obj = Objectives

This research aims to bridge these gaps and make practical and academic contributions. It offers an industry and policy-oriented framework for BSC, aiding strategic and operational decisions while considering sustainability. Strategic decisions encompass optimal facility locations and numbers, while operational decisions involve vehicle routing, vehicle numbers, biomass allocation, pellet production, and allocation. Academically, this proposed model can be adapted for both single and multi-objective scenarios, serving as a foundation for a sustainable LRP model in BSC. This model can also be utilized for any two-echelon BSC network seeking to optimize facility locations, biomass distribution, and vehicle routing. Notably, this 2ELRP model has been tailored to the specifics of BSC by quantifying pretreatment operations within the network, setting it apart from a generic 2ELRP model.

The proposed research builds upon the work of Cao et al. [4], who addressed a single-objective 2ELRP. Our model introduces several distinctions and enhancements, contributing to the formulation of an optimization model that more accurately reflects BSC scenarios. First, the present model takes a holistic approach to sustainability, addressing the multi-objective problem rather than optimizing a single economic objective function. This approach enables the model to address network optimization considering the scenarios of different sustainable goals. Notably, this research incorporates constraints concerning connection paths and facility assignments, truck load capacities, biomass and pretreated biomass flow conservation, and subtour elimination. The inclusion of additional constraints is essential as they could illustrate the interconnections among facility assignment, connecting path and vehicle loads, and biomass flows, reflecting the BSC logistical and operational processes. Additionally, the proposed BSC network encompasses pretreatment operations within the facilities, and it is included as a parameter in the model.

Our previous work provided a comprehensive review of relevant literature and investigated a single-echelon LRP within the BSC network, involving two players: mills and collection centers [54]. Based on the preceding structure, this manuscript extends the analysis to mainly examine a two-echelon BSC network, incorporating three players: mills, collection centers, and biorefineries.

3   Problem Definition and Assumptions

This section describes the proposed model's problem definition, notations, and assumptions.

3.1   Problem definition

Figure 1 depicts the key players in the examined BSC associated with palm oil: palm oil mills, collection facilities, and biorefineries. The palm oil mills serve as the primary resource sites for feedstock. In this study, the utilized feedstock is wet short fiber (WSF), obtained through the separation and sieving of EFB. To address challenges arising from dispersed resources, high humidity, and low energy density in WSF, this research suggests establishing collection facilities equipped with pelletizing technology. This technology, implemented within the collection facilities, transforms WSF into solid biofuel (pellets). Subsequently, these produced pellets are transported to the biorefineries.
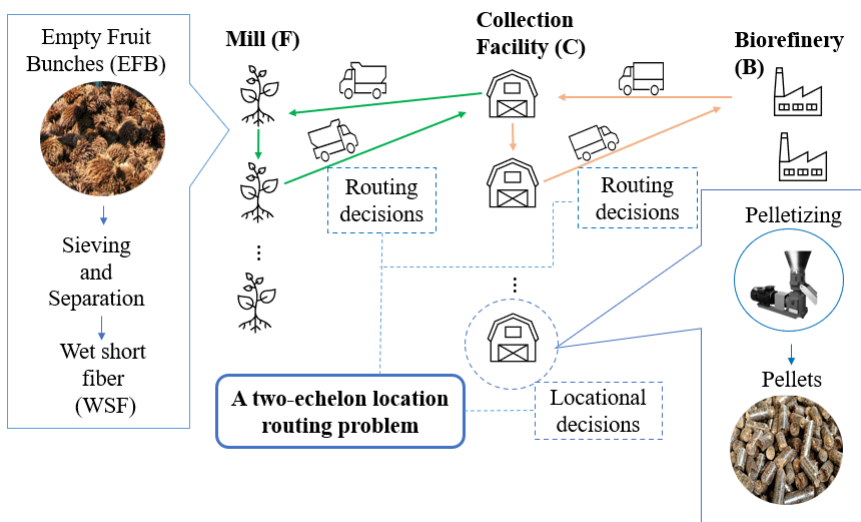

Figure 1: An overview of the investigated biomass supply chain.

Figure 2 provides a visual representation of the studied network configuration using nodes and arcs. The initial echelon network encompasses the palm oil mills and collection facilities, while the second echelon network consists of collection facilities and biorefineries. The strategic decisions pertaining to the collection facility locations are of utmost importance in shaping the network structure, impacting overall costs and the nearby population. Furthermore, the routing decisions made for trucks involved in collecting WSF and transporting pellets play a pivotal role in influencing both the total cost and CO_2 emissions.
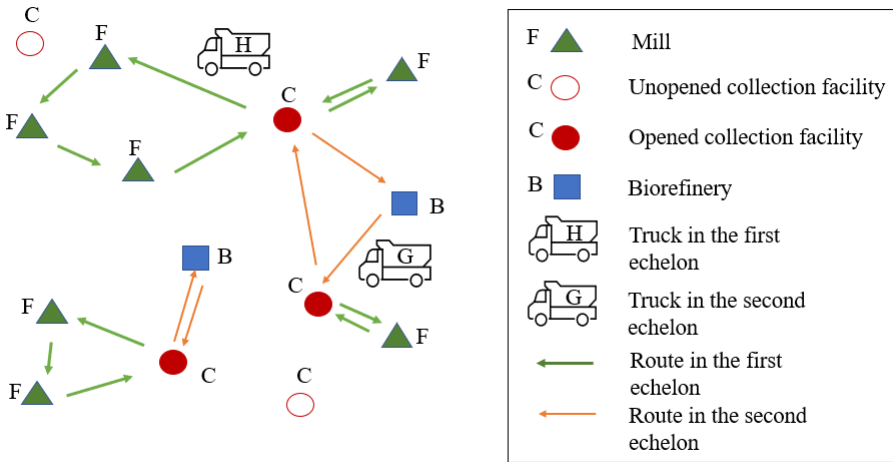
Figure 2: The depiction of the location-routing network.

The objective of this study is to optimize the simultaneous decisions regarding the locations of collection facilities and vehicle routing. This research integrates economic, social, and environmental sustainability by optimizing objective functions related to total cost, affected population, and CO_2 emissions. These combined considerations classify the research problem as a Multi-Objective Two-Echelon Location-Routing Problem (MO2ELRP). The model is formulated using Mixed-Integer Nonlinear Programming (MINLP). Notations for sets, decision variables, and parameters utilized in the model are detailed in Table 2.

Table 2: Notations used in the model.

Notation	Description
Sets	
F	Mills
C	Collection facilities
B	Biorefineries
H	Trucks in the first echelon
G	Truck in the second echelon
Decision variables	
z_i	1, if collection facility i is opened; 0, otherwise
α_{ij}	1, if mill i is assigned to collection facility j; 0, otherwise
β_{ij}	1, if collection facility i is assigned to biorefinery j; 0, otherwise.
x_{ijh}	1, if truck h travels from node i to node j; 0, otherwise
y_{ijg}	1, if truck g travels from node i to node j in the first echelon; 0, otherwise.
LP_{ijh}^F	Loading of truck h from node i to node j in the first echelon
LP_{ijg}^S	Loading of truck g from node i to node j in the second echelon
q_j^C	Quantity of biomass collected at collection facility j
q_j^{CP}	Quantity of biomass pretreated at collection facility j
Parameters	
q_i^G	Quantity of EFB produced at mill i, metric ton/day

Continued on next page

Table 2: Notations used in the model (continued).

Notation	Description
q_i^F	Quantity of WSF generated at mill i, metric tons/day
t_i^F	Capacity of mill i, metric tons FFB/hour
t_i^{CA}	Annual pretreatment capacity of collection facility i, metric tons/year
t_i^C	Daily pretreatment capacity of collection facility i, metric tons/day
t_i^B	Capacity of biorefinery i, metric tons/day
c_h^H	Capacity of truck h, metric tons
c_g^G	Capacity of truck g, metric tons
d_{ij}^F	Distance between nodes i and j in the first echelon, km
d_{ij}^S	Distance between nodes i and j in the second echelon, km
SF	Scale factor for pelletizing facilities
SZ_b	Size or capacity of a benchmark collection facility, metric tons/year
SZ_a	Size or capacity of a collection facility based on an assumption, metric tons/year
EC_b	Establishment cost for setting up a collection facility with a benchmark capacity, USD/year
EC_a	Establishment cost for setting up a collection facility based on assumed capacity, USD/year
f_i^{ECA}	Yearly cost of opening collection facility i, USD/year
f_i^{EC}	Daily cost of opening collection facility i, RM/day
f_i^{PC}	Unit cost of pretreated the biomass, RM/metric tons
e^{RH}	Fuel consumption rate of truck h in the first echelon, L/km
e^{RG}	Fuel consumption rate of truck g in the second echelon, L/km
e^P	Fuel price, RM/L
v_h^H	Transportation cost for truck h, RM/km
v_g^G	Transportation cost for truck g, RM/km
n^H	Number of trucks in the first echelon
n^G	Number of trucks in the second echelon
ρ^G	Biomass generation rate, EFB/FFB
ρ^{MO}	Rate for mulching
θ^S	Separating and sieving rate, WSF/EFB
θ^P	Pelletizing rate, pellets/WSF
γ^{Fh1}	CO_2 emission rate of truck h per kilometer, kgCO$_2$/km
γ^{Sg1}	CO_2 emission rate of truck g per kilometer, kgCO$_2$/km
γ^{Fh2}	CO_2 emission rate of truck h per metric tons per kilometer, kgCO$_2$/metric tons-km
γ^{Sg2}	CO_2 emission rate of truck g per metric tons per kilometer, kgCO$_2$/metric tons-km
Pop_i	The surrounding population at the collection facility i, people
D_j^B	Demand at biorefinery j
d^W	Number of working days
w	Daily operating hours, hour

3.2 Assumptions

To provide a structured framework for the model and establish foundational conditions for its formulation, the following assumptions are considered:

1. Open collection facilities have the capability to serve multiple mills, whereas each mill can only be associated with a single open collection facility.

2. A number of collection facilities are able to fulfill the demand of a given biorefinery, with each open collection facility being restricted to a single biorefinery assignment.

3. Within the first echelon, the vehicle routing commences at an open collection facility and concludes at the same facility after covering the assigned mills. Notably, no direct paths exist between collection facilities, and each mill must be visited exactly once.

4. In the second echelon, truck routes initiate from a biorefinery and return to the same biorefinery after visiting the designated collection facilities. No flow is permitted between biorefineries. Visitation is solely restricted to open collection facilities, and each facility must be visited only once.

5. Truck loading remains within the defined capacity of the vehicle. A homogeneous fleet of vehicles is considered.

6. The potential locations, capacities, and the populations residing in the vicinity of collection facilities are all assumed to be known.

4 Mathematical Model

This section will discuss the objective functions and constraints of the model, building upon the problem definition and the established assumptions.

4.1 The objective functions

The objective functions related to sustainable objectives encompassing three dimensions are explored. Economic performance, which has traditionally captivated the attention of numerous industry stakeholders, is quantified through the minimization of costs (1),

$$f_1 = \sum_{i \in C} f_i^{EC} \, z_i + \sum_{i \in C} f_i^{PC} \, q_i^C + \sum_{i \in F \cup C} \sum_{j \in F \cup C} \sum_{h \in H} v_h^H \, d_{ij}^F \, x_{ijh} + \sum_{i \in C \cup B} \sum_{j \in C \cup B} \sum_{g \in G} v_g^G \, d_{ij}^S \, y_{ijg}. \quad (1)$$

This equation incorporates four distinct components: the cost associated with establishing collection facilities (the initial term), the expenses linked to pretreatment (pelletizing) (the second term), and transportation costs (the third and fourth terms).

In addressing the social aspect, this study attempts to mitigate the adverse effects of facility placement on the local community. Candidate facility locations with fewer surrounding populations are preferable choices. According to (2), it is less likely that densely residential locations will be chosen for the facility establishment,

$$f_2 = \sum_{i \in C} Pop_i \, z_i. \quad (2)$$

Indirectly, the fewer individuals impacted by locational decisions, the lesser the concentration of negative social effects on the communities. This concept draws inspiration from the research conducted by Tirkolaee et al. [49], which tackled Location-Routing Problems (LRP) in other areas of application.

Addressing the environmental component, this study will concentrate on the CO_2 emissions stemming from transportation activities, assuming that emissions from pelletizing technology are negligible. The investigation will emphasize the influence of loaded and empty trucks on CO_2 emissions (3),

$$
\begin{aligned}
f_3 = &\sum_{i \in C} \sum_{j \in F} \sum_{h \in H} \gamma^{Fh1} \, d_{ij}^F \, x_{ijh} + \sum_{i \in B} \sum_{j \in C} \sum_{g \in G} \gamma^{Sg1} \, d_{ij}^S \, y_{ijg} \\
&+ \sum_{i \in F} \sum_{j \in F \cup C} \sum_{h \in H} \gamma^{Fh2} \, d_{ij}^F \, LP_{ijh}^F + \sum_{i \in C} \sum_{j \in C \cup B} \sum_{g \in G} \gamma^{Sg2} \, d_{ij}^S \, LP_{ijg}^S.
\end{aligned}
\tag{3}
$$

The first term of the equation pertains to CO_2 release linked to travel distance, applicable when trucks in the first echelon depart from collection facilities without any cargo. The second term mirrors a similar scenario involving empty trucks departing from biorefineries within the second echelon. The third term elaborates on emissions from trucks in the first echelon, considering both carrying loads and travel distance. The fourth term captures the emissions scenario of loaded trucks in the second echelon. The notion of directly correlating emissions of loaded trucks with travel distance and truck loading draws inspiration from the work of Roni et al. [34].

4.2   The first echelon constraints

The constraints applicable to the initial echelon network encompassing mills and collection facilities are outlined below. Constraint (4) guarantees that each mill is visited precisely once by a truck. Constraint (5) ensures that the total number of trucks entering and departing from mills (or collection facilities) are the same. Constraint (6) signifies that each truck can undertake the journey from a mill to a collection facility at most once.

$$
\sum_{j \in F \cup C} \sum_{h \in H} x_{ijh} = 1, \quad \forall i \in F,
\tag{4}
$$

$$
\sum_{i \in F \cup C} x_{ijh} = \sum_{i \in F \cup C} x_{jih}, \quad \forall j \in F \cup C, \quad \forall h \in H,
\tag{5}
$$

$$
\sum_{i \in F} \sum_{j \in C} x_{ijh} \leq 1, \quad \forall h \in H.
\tag{6}
$$

Constraint (7) prohibits the occurrence of loop routes for each node. Constraint (8) prevents direct connections between collection facilities within the first echelon. Constraint (9) commands that an open collection facility must serve at least one mill. Constraint (10) ensures that the total amount of WSF collected from the assigned mills should be less than the capacity of the collection

facility.

$$x_{ijh} = 0, \quad \forall i, j \in F \cup C, \quad i = j, \quad \forall h \in H, \tag{7}$$

$$\sum_{h \in H} x_{ijh} = 0, \quad \forall i, j \in C, \tag{8}$$

$$\sum_{j \in F} \sum_{h \in H} x_{ijh} \geq z_i, \qquad \forall i \in C, \tag{9}$$

$$\sum_{i \in F} q_i^F \alpha_{ij} \leq t_j^c z_j, \quad \forall j \in C. \tag{10}$$

Constraint (11) introduces the potential for a route (i, j) to exist between a mill and a collection facility if an assignment is made, whereas Constraint (12) pertains to a route (j, i). Constraint (13) serves as a constraint aimed at preventing subtours, ensuring that two mills without congruent assignments do not have a connecting route.

$$\sum_{h \in H} x_{ijh} \leq \alpha_{ij}, \quad \forall i \in F, \quad \forall j \in C, \tag{11}$$

$$\sum_{h \in H} x_{jih} \leq \alpha_{ij}, \quad \forall i \in F, \quad \forall j \in C, \tag{12}$$

$$\sum_{h \in H} x_{ijh} + \alpha_{ik} + \sum_{m \in C, m \neq k} \alpha_{jm} \leq 2, \quad \forall i, j \in F, \quad \forall k \in C. \tag{13}$$

Constraint (14) preserves the flow balance of incoming and outgoing trucks carrying loads to the amount of WSF available at each mill. Constraint (15) indicates that the carrying loads of a truck should be less than its capacity. Constraint (16) elaborates that the total loads of trucks entering a collection facility equal the amount of WSF collected from assigned mills.

$$\sum_{j \in F \cup C} \sum_{h \in H} LP_{ijh}^F - \sum_{j \in F \cup C} \sum_{h \in H} LP_{jih}^F = q_i^F, \quad \forall i \in F, \tag{14}$$

$$LP_{ijh}^F \leq c_h^H x_{ijh}, \quad \forall i, j \in F \cup C, \quad i \neq j, \quad \forall h \in H, \tag{15}$$

$$\sum_{j \in F} \sum_{h \in H} LP_{jih}^F = \sum_{j \in F} \alpha_{ji} q_j^F, \quad \forall i \in C. \tag{16}$$

Constraints (17) and (18) establish constraints on the permissible load capacities. Constraint (19) enforces that trucks must depart from the collection facility without carrying any load. Constraint (20) asserts that the quantity of WSF received by the collection facility matches the total load of trucks entering the facility. Constraint (21) pertains to the production of pretreated biomass (pellets) by the collection facility.

$$LP_{ijh}^F \leq \left(c_h^H - q_j^F \right) x_{ijh}, \quad \forall i \in F \cup C, \quad \forall j \in F, \quad \forall h \in H, \tag{17}$$

$$LP_{ijh}^F \geq q_i^F x_{ijh}, \quad \forall i \in F, \quad \forall j \in F \cup C, \quad \forall h \in H, \tag{18}$$

$$\sum_{j \in F} LP_{ijh}^F = 0, \quad \forall i \in C, \quad \forall h \in H, \tag{19}$$

$$q_j^C = \sum_{i \in F} \sum_{h \in H} LP_{ijh}^F, \quad \forall j \in C, \tag{20}$$

$$q_j^{CP} = \theta^P q_j^C, \quad \forall j \in C. \tag{21}$$

4.3   The second echelon constraints

The constraints pertaining to the second echelon network involving collection facilities and biorefineries are outlined as follows. Constraint (22) ensures that an open collection facility is visited exactly once. Constraint (23) commands that a biorefinery can only be connected to a collection facility if the collection facility is operational. Constraint (24) guarantees that at least one truck travels from a collection facility to each biorefinery. Constraint (25) maintains the balance between the number of trucks entering and leaving a collection facility (or biorefinery). Constraint (26) stipulates that each truck can make the journey from a biorefinery to a collection facility at most once.

$$\sum_{j\in C\cup B}\sum_{g\in G} y_{ijg} = z_i, \quad \forall i \in C, \tag{22}$$

$$y_{ijg} \leq z_j, \quad \forall i \in B, \quad \forall j \in C, \quad \forall g \in G, \tag{23}$$

$$\sum_{g\in G}\sum_{j\in C} y_{ijg} \geq 1, \quad \forall i \in B, \tag{24}$$

$$\sum_{j\in C\cup B} y_{ijg} = \sum_{j\in C\cup B} y_{jig}, \quad \forall i \in B \cup C, \quad \forall g \in G, \tag{25}$$

$$\sum_{i\in B}\sum_{j\in C} y_{ijg} \leq 1, \quad \forall g \in G. \tag{26}$$

Constraint (27) prohibits the occurrence of loop routes. Constraint (28) signifies the absence of direct connections between biorefineries within the second echelon. Constraint (29) dictates that an open collection facility can only be allocated to a single biorefinery. Constraint (30) guarantees that the quantity of pellets collected from the designated collection facilities remains within the capacity of the biorefinery.

$$y_{ijg} = 0, \quad \forall i,j \in B \cup C, \quad i = j, \quad \forall g \in G, \tag{27}$$

$$\sum_{g\in G} y_{ijg} = 0, \quad \forall i,j \in B, \tag{28}$$

$$\sum_{j\in B} \beta_{ij} = z_i, \quad \forall i \in C, \tag{29}$$

$$\sum_{i\in C} q_i^{CP} \beta_{ij} \leq t_j^B, \quad \forall j \in B. \tag{30}$$

Constraint (31) establishes the potential for a route (i,j) to exist when a collection facility is assigned to a biorefinery, while Constraint (32) employs a similar concept for the route (j,i). The subtour elimination constraint (Constraint (33)) eliminates the connection path between two collection facilities if they are assigned to different biorefineries.

$$\sum_{g\in G} y_{ijg} \leq \beta_{ij}, \quad \forall i \in C, \quad \forall j \in B, \tag{31}$$

$$\sum_{g\in G} y_{jig} \leq \beta_{ij}, \quad \forall i \in C, \quad \forall j \in B, \tag{32}$$

$$\sum_{g\in G} y_{ijg} + \beta_{ik} + \sum_{m\in B, m\neq k} \beta_{jm} \leq 2, \quad \forall i,j \in C, \quad \forall k \in B. \tag{33}$$

Constraint (34) is the flow conservation constraint for pellets produced at the collection facility. Constraint (35) indicates the carrying loads of a truck should not be more than the capacity of the truck. Constraints (36) and (37) are the bounding constraints for the truck's carrying loads. Constraint (38) reflects that a truck is empty when it departs from a biorefinery.

$$\sum_{j \in C \cup B} \sum_{g \in G} LP_{ijg}^S - \sum_{j \in C \cup B} \sum_{g \in G} LP_{jig}^S = q_i^{CP}, \forall i \in C, \tag{34}$$

$$LP_{ijg}^S \leq c_g^G y_{ijg}, \quad \forall i,j \in C \cup B, \quad i \neq j, \quad \forall g \in G, \tag{35}$$

$$LP_{ijg}^S \leq \left(c_g^G - q_j^{CP}\right) y_{ijg}, \quad \forall i \in C \cup B, \quad \forall j \in C, \quad \forall g \in G, \tag{36}$$

$$LP_{ijg}^S \geq q_i^{CP} y_{ijg}, \quad \forall i \in C, \quad \forall j \in C \cup B, \quad \forall g \in G, \tag{37}$$

$$\sum_{j \in C} LP_{ijg}^S = 0, \quad \forall i \in B, \quad \forall g \in G. \tag{38}$$

Constraint (39) shows the pellets received by a biorefinery equals the total carrying loads of trucks entering the biorefinery. Constraint (40) ensures the demand for a biorefinery must be met. Constraints (41) to (49) are the constraints for the decision variables.

$$q_j^B = \sum_{i \in C} \sum_{g \in G} LP_{ijg}^S, \quad \forall j \in B, \tag{39}$$

$$q_j^B \geq D_j^B, \quad \forall j \in B, \tag{40}$$

$$z_i \in \{0,1\}, \quad \forall i \in C, \tag{41}$$

$$\alpha_{ij} \in \{0,1\}, \quad \forall i \in F, \quad \forall j \in C, \tag{42}$$

$$\beta_{ij} \in \{0,1\}, \quad \forall i \in C, \quad \forall j \in B, \tag{43}$$

$$x_{ijh} \in \{0,1\}, \quad \forall i,j \in F \cup C, \quad \forall h \in H, \tag{44}$$

$$y_{ijg} \in \{0,1\}, \quad \forall i,j \in C \cup B, \quad \forall g \in G, \tag{45}$$

$$LP_{ijh}^F \geq 0, \quad \forall i,j \in F \cup C, \quad \forall h \in H, \tag{46}$$

$$LP_{ijg}^S \geq 0, \quad \forall i,j \in C \cup B, \quad \forall g \in G, \tag{47}$$

$$q_j^C \geq 0, \quad \forall j \in C, \tag{48}$$

$$q_j^{CP} \geq 0, \quad \forall j \in C. \tag{49}$$

4.4 Multi-objective optimization

This study employs the weight sum approach to integrate all objective functions ($f_i, i = 1, 2, 3$) into a single composite function. Given that the units of the objective functions ($f_i, i = 1, 2, 3$) may vary, the study individually optimizes each objective function to determine its optimal value ($f_i^*, i = 1, 2, 3$). (50) transforms the objective function (Mf) into a dimensionless unit by dividing the weighted objective functions ($\omega_i f_i$) by their respective optimum values (f_i^*).

$$Mf = \sum_i \frac{\omega_i f_i}{f_i^*}, \quad i = 1, 2, 3. \tag{50}$$

It is important to note that this research assumes equal importance for each objective, implying that all weights are equal.

5 Results and Discussion

This section focuses on the computational results aimed at assessing the proposed MO2ELRP model. Computational experiments were carried out on a test case involving nine mills, five potential collection facilities, and two biorefineries. The objective was to validate the model's capacity to adapt its strategies concerning facility placements, truck routing, and assignments in accordance with varying sustainable objectives. The test instance was generated using data pertaining to palm oil biomass and information regarding pelletizing technology.

5.1 Data and parameter setting

Table 3 shows the processing capacities of mills, with data obtained from Lam et al. [18]. Table 4 outlines the parameters for biomass. The biomass generation rate $\left(\rho^G\right)$ defines that 0.234 metric tons of EFB is produced from every metric of fresh fruit bunches (FFB). Using the information in Table 3 and assuming that the mills are working 16 hours per day (w), the daily amount of EFB generated in mills could be calculated using (51),

$$q_i^G = t_i^F \rho^G w, \quad \forall i \in F. \tag{51}$$

Table 3: The mills information.

Mill	Cartesian coordinates	Processing capacity $\left(t_i^F\right)$ (metric tons FFB/hour) [18]
F1	$(8, 29)$	55
F2	$(10, 40)$	100
F3	$(20, 20)$	80
F4	$(35, 78)$	90
F5	$(38, 67)$	35
F6	$(68, 66)$	70
F7	$(66, 85)$	80
F8	$(100, 54)$	100
F9	$(120, 50)$	60

Table 4: Parameters for biomass.

Parameter	Value	Reference
ρ^G	0.234 EFB/FFB	[18]
ρ^{MO}	0.9	Assumption
θ^S	0.24 WSF/EFB	[18]
θ^P	0.33 pellets/WSF	[18]

In current practice, the EFB is directly used as mulch [26] or co-compositing with palm oil mill effluents before mulching [8, 16]. Consequently, this study proposes utilizing a modest portion

of EFB for biofuel conversion to minimize any substantial impact on the current practices within the palm oil industry. This study assumes that the mulching rate $\left(\rho^{MO}\right)$ will be adjusted to 0.9 which means 90% of generated EFB in mills will be used for mulching at the plantation. The EFB that remains will then be subjected to a separation and sieving procedure, characterized by a rate denoted as $\left(\theta^S\right)$, quantified at 0.24. This process yields wet short fiber (WSF) which serves as the crucial feedstock for subsequent biofuel conversion. The rate signifies that for every metric ton of EFB processed, 0.24 metric tons of WSF are generated. The availability of WSF at each mill can be obtained using (52),

$$q_i^F = \theta^S \left(1 - \rho^{MO}\right) q_i^G, \qquad \forall i \in F. \tag{52}$$

Subsequently, the pelletizing technology with a rate $\left(\theta^P\right)$ of 0.33 at the collection facility is employed to pretreat the WSF. This rate denotes that for each metric ton of WSF processed, 0.33 metric tons of pellets (solid biofuel) are generated.

Table 5 presents the establishment cost for a collection facility equipped with pelletizing technology. The information for the 300,000 metric tons/year (SZ_b) facility serves as the reference value for calibrating the establishment cost. In this study, it is assumed that the capacity of all candidate collection facilities is 7,500 metric tons/year $\left(SZ_a, t_i^{CA}\right)$.

Table 5: The yearly opening cost of a facility with pelletization.

Parameter	Value	Reference/ Note
SZ_b	300,000 metric tons/year	Reference Value (Base) [19]
EC_b	3,476,219 USD /year	
SZ_a , t_i^{CA}	7,500 metric tons/year	Assumption
EC_a , f_i^{ECA}	380,076.6015 USD/year	Obtained using (53)

(53) [47] computes the establishment cost by adjusting the base capacity value to another using a scale factor of 0.6 (SF) for pelletizing facilities [24],

$$\frac{EC_a}{EC_b} = \left(\frac{SZ_a}{SZ_b}\right)^{SF}. \tag{53}$$

Table 6: Parameters for the collection facilities.

Parameter	Value	Note
t_i^C	25 metric tons/day	Obtained using (54)
f_i^{EC}	USD 1266.922 or RM 5574.46*	Obtained using (55)
f_i^{PC}	RM 176/metric tons	Assumption

*Currency rate: 1 USD = RM4.40 (dated at 31 December 2022)

Table 6 lists the parameters associated with the collection facilities. Assuming 300 working days per year $\left(d^W\right)$, (54) calculates the daily pelletizing capacity, while (55) computes the daily estab-

lishment cost,

$$t_i^C = \frac{t_i^{CA}}{d^W}, \tag{54}$$

$$f_i^{EC} = \frac{f_i^{ECA}}{d^W}. \tag{55}$$

Table 7 shows the data related to the candidate collection facilities and their respective population density, while Table 8 lists the demand for biorefineries.

Table 7: The locations of candidate collection facilities and their population.

Collection Facility	Cartesian Coordinates	Population(Pop_i) (People)
C10	(25, 35)	7964
C11	(45, 85)	8109
C12	(55, 75)	4208
C13	(110, 40)	5263
C14	(118, 23)	4928

Table 8: The demand of biorefineries.

Biorefinery	Cartesian coordinates	Demand $\left(D_j^B\right)$ (metric ton/day)
B15	(31, 50)	14
B16	(100, 27)	4

Tables 9 and 10 denote the information and parameters for the trucks. The trucks ($\forall h \in H, \forall g \in G$) in this study are homogenous, where their capacities $\left(c_h^H, c_g^G\right)$ in both echelons are 15 metric tons.

Table 9: Information related to the trucks of 15 metric tons.

Fuel Information	Value	Reference
e^{RH}, e^{RG}	0.261 L/km	[14]
e^P	RM 2.15 /L	[29]

Table 10: Parameters for the trucks.

Parameter	Value	Reference/ Note
c_h^H, c_g^G	15 metric tons	[14]
v_h^H, v_g^G	RM 0.5612/km	Obtained using (56) and (57)
$\gamma^{Fh1}, \gamma^{Sg1}$	0.6786 kg/km	[14]
$\gamma^{Fh2}, \gamma^{Sg2}$	0.41243 kg/metric ton-km	[11]

Equations (56) and (57) are used to obtain the transportation costs $\left(v_h^H, v_g^G\right)$ for both echelons. Equations (58) and (59) denote the number of trucks $\left(n^H, n^G\right)$ in the first and second echelons, respectively. The emission rate of CO_2 for an empty truck is 0.6786 kg CO_2 per km $\left(\gamma^{Fh1}, \gamma^{Sg1}\right)$ [14], whereas for a loaded truck, it is 0.41243 kg CO_2 per metric ton per kilometer $\left(\gamma^{Fh2}, \gamma^{Sg2}\right)$ [11].

$$v_h^H = \left(e^{RH}\right)\left(e^P\right), \tag{56}$$

$$v_g^G = \left(e^{RG}\right)\left(e^P\right), \tag{57}$$

$$n^H = 2\left\lceil \frac{\sum_{i \in M} q_i^F}{c_h^H} \right\rceil, \tag{58}$$

$$n^G = 2\left\lceil \frac{\theta^P \sum_{i \in M} q_i^F}{c_g^G} \right\rceil. \tag{59}$$

5.2 Result analysis

The MINLP model in this study was solved using the General Algebraic Modeling System (GAMS) with the DICOPT optimizer solver. Initially, computational experiments were performed by solving the model for each individual objective function. This was done to attain the optimal solution for each dimension of sustainability and to validate the model's ability to adapt its strategy accordingly. Subsequently, multi-objective optimization was carried out using the weighted sum approach.
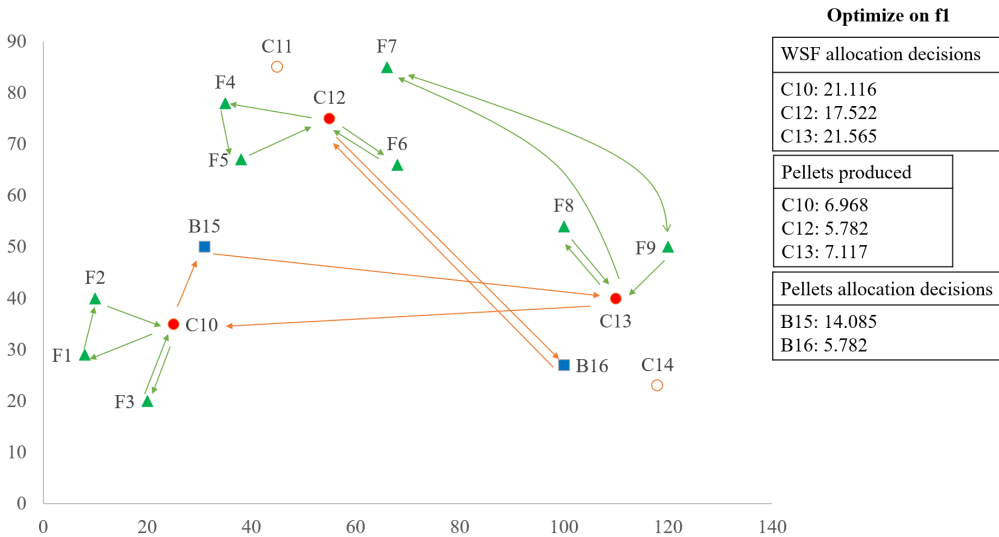

Figure 3: Network of optimizing the first objective function.

Figure 3 illustrates the network structure of optimizing economic performance (total cost minimization). The model suggests opening three collection facilities, C10, C12, and C13. Table 11 reports the assignment to these open collection facilities. The mills F1, F2, and F3 are assigned to C10 in the first echelon. F4, F5, and F6 supply the feedstock for C12. The remaining mills are assigned to C13. The demand for biorefinery B15 in the second echelon is satisfied by C10 and C13, while C12 is assigned to B16. Figure 3 shows that C10, C12, and C13 will be allocated 21.116

metric tons, 17.522 metric tons, and 21.565 metric tons of WSF, respectively. According to the allocation, C10, C12, and C13 will each generate 6.968 metric tons, 5.782 metric tons, and 7.112 metric tons of pellets. Pellets will then be delivered to B15 and B16 in quantities of 14.085 and 5.782 tons, respectively.

Figure 3 and Table 11 demonstrate that the first echelon requires six trucks, and the second requires two trucks to transport the WSF and pellets. Table 11 also provides information regarding the trucks' routing and carrying loads. The configuration of C10-F1-F2-C10 (0-4.942-13.928) describes the details of a truck activity. It means that an empty truck departs from C10 to visit F1. Then, the truck leaves F1 and carries a load of 4.942 metric tons to visit F2. Next, the truck collects the WSF from F2, increasing the loads to 13.928 metric tons. Lastly, the truck completes its trip and returns to the initial collection facility, C10.

Figure 4 illustrates that in the network structure designed to minimize the total population impact, C10 and C12 are retained. However, for this network, C14 proves to be a better location than C13. Under this configuration, C10, C12, and C14 will receive 17.522 metric tons, 17.971 metric tons, and 24.741 metric tons of WSF, respectively, and produce 5.782, 5.930, and 8.154 metric tons of pellets, respectively. Additionally, 14.085 metric tons of pellets are transported from C12 and C14 to B15, while B16 receives all the pellets produced by C10. Table 11 shows that this network design also requires six trucks and two trucks for the first and second echelons, respectively.
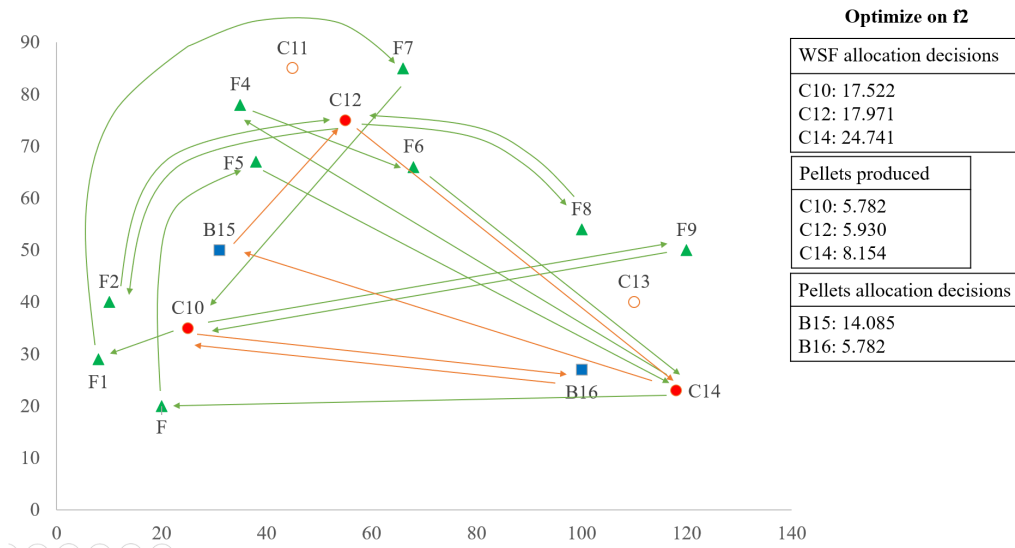

Figure 4: Network of optimizing the second objective function.

Table 11: The optimal solutions for the different objective functions.

Optimize	First Echelon Decisions	Second Echelon Decisions
f_1	[a]C10: F1, F2, F3 [b](21.116, 6.968)	[d]B15: C10, C13 [e](14.085)
	C12: F4, F5, F6 (17.522, 5.782)	B16: C12 (5.782)
	C13: F7, F8, F9 (21.565, 7.117)	
	[c]C10-F1-F2-C10 (0-4.942-13.928)	[f]B15-C13-C10-B15 (0-7.117-14.085)
	C10-F3-C10 (0-7.189)	B16-C12-B16 (0-5.782)
	C12-F4-F5-C12 (0-8.087-11.232)	
	C12-F6-C12 (0-6.29) C13-F8-C13 (0-8.896)	
	C13-F7-F9-C13 (0-7.189-12.58)	
f_2	C10: F1, F7, F9 (17.522, 5.782)	B15: C12, C14 (14.085)
	C12: F2, F8 (17.971, 5.930)	B16: C10 (5.782)
	C14: F3, F4, F5, F6 (24.741, 8.154)	
	C10-F1-F7-C10 (0-4.942-12.131)	B15-C12-C14-B15 (0-5.93-14.085)
	C10-F9-C10 (0-5.391) C12-F2-C12 (0-8.986)	B16-C10-B16 (0-5.782)
	C12-F8-C12 (0-8.986)	
	C14-F3-F5-C14 (0-7.189-10.334)	
	C14-F4-F6-C14 (0-8.087-14.377)	
f_3	C10: F1, F2, F3 (21.116, 6.968)	B15: C10, C11, C12 (15.123)
	C11: F4, F5 (11.232, 3.707)	B16: C13 (4.744)
	C12: F6, F7 (13.478, 4.448)	
	C13: F8, F9 (14.377, 4.744)	
	C10-F1-C10 (0-4.942) C10-F2-C10 (0-8.986)	B15-C11-C12-B15 (0-3.707-8.154)
	C10-F3-C10 (0-7.189)	B15-C10-B15 (0-6.968)
	C11-F5-F4-C11 (0-3.145-11.232)	B16-C13-B16 (0-4.744)
	C12-F6-C12 (0-6.29) C12-F7-C12 (0-7.189)	
	C13-F8-C13 (0-8.986) C13-F9-C13 (0-5.391)	
Mf	C10: F2, F3, F4 (24.261, 8.006)	B15: C10, C12 (14.085)
	C12: F1, F6, F7 (18.421, 6.079)	B16: C13 (5.782)
	C13: F5, F8, F9 (17.521, 5.782)	
	C10-F2-C10 (0-8.986) C10-F3-C10 (0-7.189)	B15-C10-B15 (0-8.006)
	C10-F4-C10 (0-8.087) C12-F1-C12 (0-4.942)	B15-C12-B15 (0-6.079)
	C12-F6-C12 (0-6.290) C12-F7-C12 (0-7.189)	B16-C13-B16 (0-5.782)
	C13-F5-F8-C13 (0-3.145-12.131)	
	C13-F9-C13 (0-5.391)	

Note:
(a) "C10: F1, F2, F3" denotes that the facility placement at location C10, with F1, F2, and F3 assigned to it.
(b) "(21.116, 6.968)" indicates that the facility will receive 21.116 metric tons of WSF and produce 6.968 metric tons of pellets.
(c) "C10-F1-F2-C10 (0-4.942-13.928)" means that the route begins from C10 with zero load, travels to F1 to pick up 4.942 metric tons of WSF, then proceeds to F2, and ends the route back to C10 with a total load of 13.928 metric tons of WSF.
(d) "B15: C10, C13" denotes that B15 are assigned with C10 and C13.
(e) "(14.085)" indicates that the biorefinery receives 14.085 metric tons of pellets.
(f) "B15-C13-C10-B15 (0-7.117-14.085)" indicates the truck starts from B15 without any load, transports 7.117 metric tons of pellets from C13, then travels to C10 and returns to B15 with a total load of 14.085 metric tons of pellets.

Figure 5 shows that the model increases the collection facilities to four, C10, C11, C12, and C13 with CO_2 emissions as the objective function. As a reminder, the third objective function relates to distance and truck carrying loads, which necessitates the inclusion of four collection facilities to minimize travel distance. Consequently, more trucks are required to reduce their cargo loads (Table 11). Thus, the first echelon requires eight trucks, and the second echelon requires three trucks. Figure 5 also reveals that C11 will receive the least amount of WSF (11.232 metric tons) and produce the lowest quantity of pellets (3.707 metric tons). C10 receives nearly double the amount of WSF compared to C11 and produces a corresponding quantity of pellets. C12 and C13 generate 4.448 metric tons and 4.744 metric tons of pellets, respectively, from the WSF they receive. B15 will receive 15.123 metric tons of pellets produced by C10, C11, and C12, while B16 will receive all the pellets produced by C13.
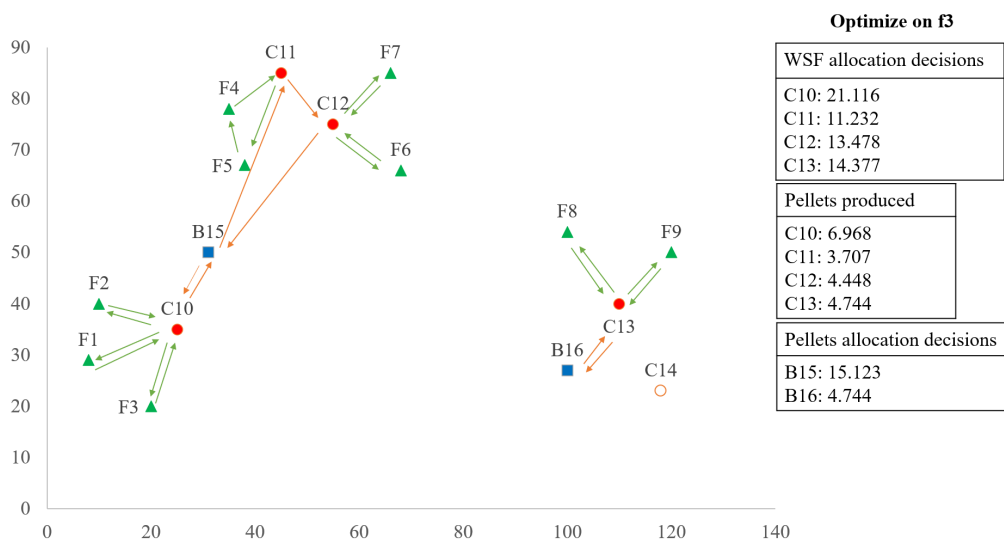
Figure 5: Network of optimizing the third objective function.

The findings presented in Table 12 highlight the inherent trade-offs between the proposed objective functions. Improving one goal often comes at the expense of compromising other goals. When the model is oriented towards cost minimization, it incurs a daily cost of RM27682.332, but this decision impacts 17435 individuals and releases 1355.644 kg CO_2 per day. On the other hand, optimizing the second objective function for the social dimension can reduce the total affected population to 17100 people, but it leads to the release of a maximum of 3411.008 kg CO_2. Furthermore, this network increases expenses by 1.46%, slightly higher than the network aimed at minimizing the total cost. When the model aims to reduce CO_2 emissions , it significantly cuts CO_2 emissions to 747.122 kg CO_2 per day. However, the economic and social implications may not be positive as it incurs the highest cost of RM33128.188 per day and impacts the highest number of people, totaling 25544 individuals.

Table 12: The values of objective functions.

Function	Total Cost (RM)	Total Population (People)	Total CO_2 emissions (kg)	Composite Value
f_1	**27682.332**	17435	1355.644	-
f_2	28086.722	**17100**	3411.008	-
f_3	33128.188	25544	**747.122**	-
Mf	27692.182	17435	1075.14	3.66

Subsequently, this study examines how the model adjusts its facility establishment and truck routing strategies when optimizing multi-objective functions. Figure 6 illustrates that opening C10, C12, and C13 is the most favorable strategic decision when all objective functions are equally important. C10, as the largest receiver of WSF, produces 8.006 metric tons of pellets from 24.261 metric tons of WSF. C12 and C13 convert 18.241 metric tons and 17.521 metric tons of WSF into 6.079 metric tons and 5.782 metric tons of pellets, respectively. Subsequently, B16 collects all the pellets produced by C13, while the pellets produced by C12 and C10 meet the demand of B15. Since optimizing environmental performance is also one of the goals, the model suggests employing 11 trucks and advocates for reduced truck carrying loads (Table 11).

The results of the performance indices presented in Table 12 also underscore the benefits of concurrently optimizing multiple objective functions. Despite the daily expenses amounting to RM27692.182, it is only 0.036% more costly than the network optimized solely for economic performance. This slight increase can be interpreted as the cost of a network that simultaneously considers CO_2 emissions and their adverse social impact. Similarly, this network structure impacts 17435 individuals, slightly more than the model focused solely on minimizing the total population (f_2), but better than the model optimized for the third objective function (f_3). From the perspective of reducing CO_2 emissions, the CO_2 emissions from the multi-objective optimization network rank as the second lowest.
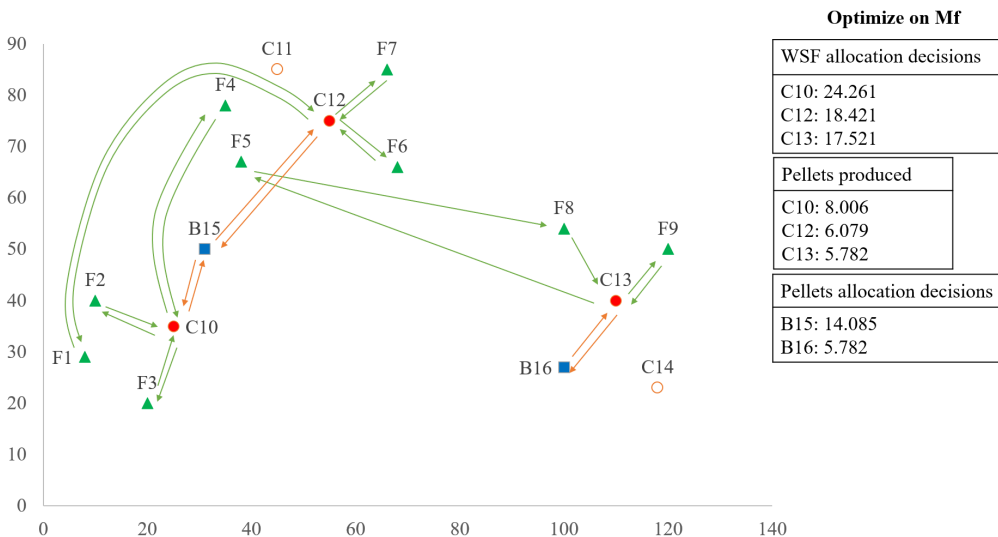

Figure 6: Network of optimizing the multi-objective functions.

5.3   Sensitivity analysis

A sensitivity analysis was undertaken to assess the impact of certain parameters (results from multi-objective optimization using the weighted sum approach). Three parameters were selected for analysis: transportation cost, CO_2 emission rates, and collection facility capacity. These parameters were varied within a range of [-40%, 40%] with increments of 10% to evaluate the impact of the uncertainty in parameter values on the supply chain network configuration and decisions (decision variables). Figures 7, 8, and 9 show the effects of parameter value uncertainty on the objective functions within the examined ranges and results with significant changes, specifically at -40% and +40%, are highlighted in Tables 13, 14, and 15.

Figure 7 depicts that the objective functions of total cost and total CO_2 emissions are responsive to changes in transportation cost, whereas the objective function of total population remains unaffected by this parameter. As anticipated, transportation cost parameter significantly influences the total expenditure in the supply chain: a decrease in transportation cost by -40% results in a 0.59% reduction in total cost, while an increase of 40% leads to a 0.42% rise in total cost. Transportation costs are primarily influenced by fuel prices and the fuel consumption rate of trucks. Since fuel price is subject to uncontrollable factors like global market supply and demand, focus should be directed towards truck fuel consumption rate. Utilizing fuel-efficient trucks and ensuring regular maintenance and servicing are advisable measures to mitigate fuel consumption. Older trucks or those lacking proper maintenance tend to consume more fuel, thereby increasing supply chain costs. Meanwhile, the fluctuation of total CO_2 emissions does not exhibit a predictable pattern despite its sensitivity to the transportation cost parameter.
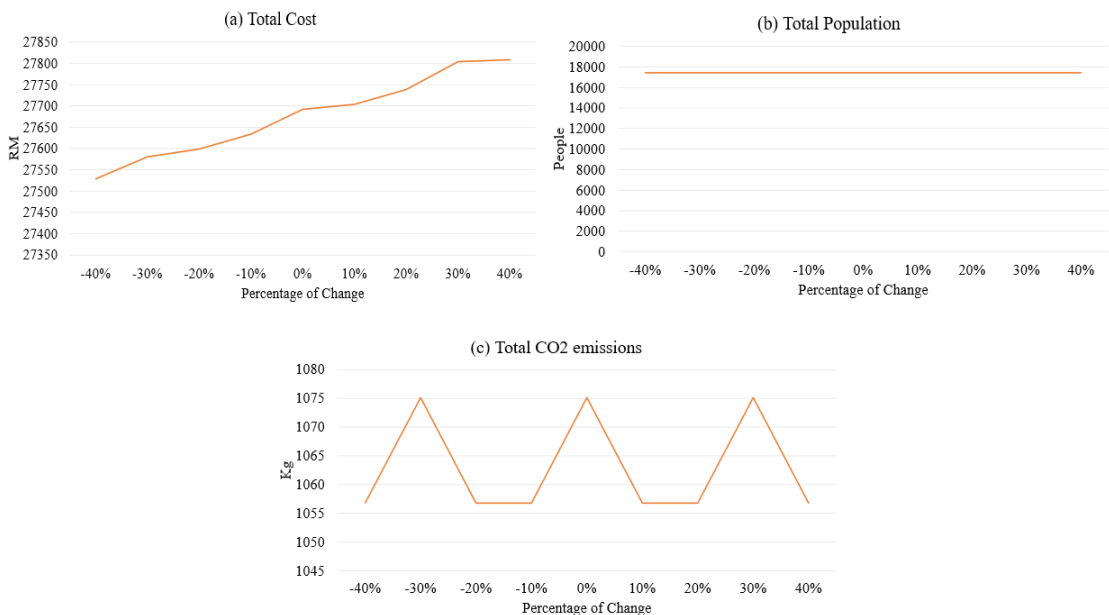

Figure 7: Effect of the transportation cost on the objective functions: (**a**) The first objective function. (**b**) The second objective function. (**c**) The third objective function.

Table 13 illustrates the impact of varying transportation costs by -40% and 40% on network decisions. The sensitivity analysis reveals that changes in transportation costs do not affect locational decisions, with C10, C12, and C13 consistently chosen for facility placement. Despite variations

in the transportation cost parameter, constraints imposed by facility capacities, truck availability, and demand lead to relatively consistent network configurations. While there are minor adjustments in the assignment, routing, biomass allocation, and pellet production decisions (decision variables), the number of routes in the first echelon remains constant at eight trucks, fully utilizing available resources. Similarly, decisions in the second echelon exhibit minimal variation across scenarios, indicating limited sensitivity to transportation cost changes. This suggests that while the uncertainty in transportation costs may influence certain decisions, locational choices remain largely unaffected.

Figure 8 illustrates that the total CO_2 emissions is significantly influenced by changes in CO_2 emission rates. A decrease of 40% leads to a reduction in total CO_2 emissions by 39.99%, while an increase of 40% results in a corresponding rise. The condition of trucks plays a crucial role in CO_2 emissions, with aging trucks emitting more CO_2 due to exhaust from old engines and higher fuel consumption. Additionally, the type of fuels used also affects CO_2 emission rates. It is suggested that truck conditions and fuel types are the areas to be monitored in the supply chain to achieve CO_2 emission reduction objectives. Table 14 illustrates the impact on network configurations when the CO_2 emission rate was varied by -40% and 40%. Interestingly, the results of decision variables show no sensitivity to changes in CO_2 emission rates, with locational, allocation, production, and routing decisions remaining consistent with the original emission rates. The rising trend of total CO_2 emissions depicted in Figure 8 is solely attributed to the increase in CO_2 emission rates.
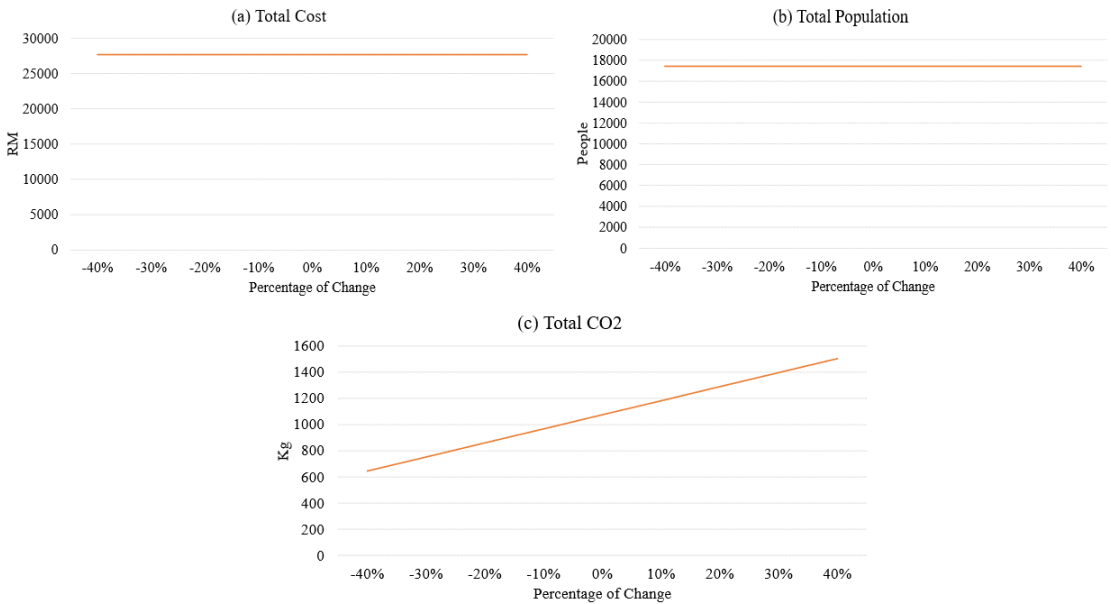

Figure 8: Effect of the CO_2 emission rates on the objective functions: (**a**) The first objective function. (**b**) The second objective function. (**c**) The third objective function.

Table 13: Effect of the transportation cost on network decisions.

Optimize	First Echelon Decisions	Second Echelon Decisions
-40%	C10: F1, F2, F3, F5 (24.261, 8.006) C12: F4, F7, F9 (20.667, 6.820) C13: F6, F8 (15.276, 5.041) C10-F1-F2-C10 (0-4.942-13.928) C10-F3-C10 (0-7.189) C10-F5-C10 (0-3.145) C12-F4-C12 (0-8.087) C12-F7-C12 (0-7.189) C12-F9-C12 (0-5.391) C13-F6-C13 (0-6.29) C13-F8-C13 (0-8.986)	B15: C10, C12 (14.826) B16: C13 (5.041) B15-C10-B15 (0-8.006) B15-C12-B15 (0-6.820) B16-C13-B16 (0-5.041)
0%	[a]C10: F2, F3, F4 [b](24.261, 8.006) C12: F1, F6, F7 (18.241, 6.079) C13: F5, F8, F9 (17.522, 5.782) [c]C10-F2-C10 (0-8.986) C10-F3-C10 (0-7.189) C10-F4-C10 (0-8.087) C12-F1-C12 (0-4.942) C12-F6-C12 (0-6.290) C12-F7-C12 (0-7.189) C13-F5-F8-C13 (0-3.145-12.131) C13-F9-C13 (0-5.391)	[d]B15: C10, C12 [e](14.085) B16: C13 (5.782) [f]B15-C10-B15 (0- 8.006) B15-C12-B15 (0-6.079) B16-C13-B16 (0-5.782)
40%	C10: F1, F2, F3, F5 (24.261, 8.006) C12: F4, F7, F9 (20.667, 6.820) C13: F6, F8 (15.276, 5.041) C10-F1-F2-C10 (0-4.942-13.928) C10-F3-C10 (0-7.189) C10-F5-C10 (0-3.145) C12-F4-C12 (0-8.087) C12-F7-C12 (0-7.189) C12-F9-C12 (0-5.391) C13-F6-C13 (0-6.29) C13-F8-C13 (0-8.986)	B15: C10, C12 (14.826) B16: C13 (5.041) B15-C10-B15 (0-8.006) B15-C12-B15 (0-6.820) B16-C13-B16 (0-5.041)

Note:
(a) "C10: F2, F3, F4" denotes that the facility placement at location C10, with F2, F3, and F4 assigned to it.
(b) "(24.261, 8.006)" indicates that the facility will receive 24.261 metric tons of WSF and produce 8.006 metric tons of pellets.
(c) "C10-F2-C10 (0-8.986)" means that the route begins from C10 with zero load, travels to F2, and ends the route back to C10 with a load of 8.986 metric tons of WSF.
(d) "B15: C10, C12" denotes that B15 are assigned with C10 and C12.
(e) "(14.085)" indicates that the biorefinery receives 14.085 metric tons of pellets.
(f) "B15-C10-B15 (0- 8.006)" indicates the truck starts from B15 without any load, transports 8.006 metric tons of pellets from C10, and returns to B15.

Table 14: Effect of the transportation cost on network decisions.

Optimize	First Echelon Decisions	Second Echelon Decisions
-40%	Decisions same as the original CO_2 emission rates (0%)	
0%	[a]C10: F2, F3, F4 [b](24.261, 8.006) C12: F1, F6, F7 (18.241, 6.079) C13: F5, F8, F9 (17.522, 5.782)	[d]B15: C10, C12 [e](14.085) B16: C13 (5.782)
	[c]C10-F2-C10 (0-8.986) C10-F3-C10 (0-7.189) C10-F4-C10 (0-8.087) C12-F1-C12 (0-4.942) C12-F6-C12 (0-6.290) C12-F7-C12 (0-7.189) C13-F5-F8-C13 (0-3.145-12.131) C13-F9-C13 (0-5.391)	[f]B15-C10-B15 (0- 8.006) B15-C12-B15 (0-6.079) B16-C13-B16 (0-5.782)
40%	Decisions same as the original CO_2 emission rates (0%)	

Note:
(a) "C10: F2, F3, F4" denotes that the facility placement at location C10, with F2, F3, and F4 assigned to it.
(b) "(24.261, 8.006)" indicates that the facility will receive 24.261 metric tons of WSF and produce 8.006 metric tons of pellets.
(c) "C10-F2-C10 (0-8.986)" means that the route begins from C10 with zero load, travels to F2, and ends the route back to C10 with a load of 8.986 metric tons of WSF.
(d) "B15: C10, C12" denotes that B15 are assigned with C10 and C12.
(e) "(14.085)" indicates that the biorefinery receives 14.085 metric tons of pellets.
(f) "B15-C10-B15 (0- 8.006)" indicates the truck starts from B15 without any load, transports 8.006 metric tons of pellets from C10, and returns to B15.

Figure 9 illustrates that the capacity of collection facilities profoundly affects all objective functions. Reducing the capacity of collection facilities necessitates opening more facilities to collect biomass. A 40% decrease in facility capacities leads to a 40.46% increase in total costs, as the need for more facilities results in higher establishment costs. Additionally, increased facility openings cause more people affected by locational decisions and might have higher CO_2 emissions due to the need for additional trucks. Conversely, the total cost and total affected people stay stagnant with the capacity increment. The total CO_2 emissions decrease until they reach a 20% increment in capacity and then remain stable.

Figure 9: Effect of the collection facility capacity on the objective functions: (**a**) The first objective function. (**b**) The second objective function. (**c**) The third objective function.

Table 15 presents the impact of collection facility capacity on network decisions. The analysis reveals that all decisions, including locational, allocation, and routing, are responsive to changes in capacity. In the scenario of a 40% capacity increment, C10, C12, and C13 also emerge as preferred facility locations, but with different assignment, allocation, and routing decisions. A drastic reduction of 40% in capacity requires all potential locations to open facilities. The sensitivity analysis reveals that all decisions (decision variables) are responsive to the uncertainty in the facility capacity parameter.

Table 15: Effect of the transportation cost on network decisions.

Optimize	First Echelon Decisions	Second Echelon Decisions
-40%	C10: F1, F2 (13.928, 4.596) C11: F4, F6 (14.377, 4.744) C12: F3, F7 (14.377, 4.744) C13: F8, F9 (14.377, 4.744) C14: F5 (3.145, 1.038)	B15: C10, C11, C12 (14.085) B16: C13, C14 (5.782)
	C10-F1-F2-C10 (0-4.942-13.928) C11-F4-C11 (0-8.087) C11-F6-C11 (0-6.290) C12-F3-C12 (0-7.189) C12-F7-C12 (0-7.189) C13-F8-C13 (0-8.986) C13-F9-C13 (0-5.391) C14-F5-C14 (0-3.145)	B15-C10-B15 (0-4.596) B15-C11-B15 (0-4.744) B15-C12-B15 (0-4.744) B16-C14-C13-B16 (1.038-5.782)
0%	[a]C10: F2, F3, F4 [b](24.261, 8.006) C12: F1, F6, F7 (18.241, 6.079) C13: F5, F8, F9 (17.522, 5.782)	[d]B15: C10, C12 [e](14.085) B16: C13 (5.782)
	[c]C10-F2-C10 (0-8.986) C10-F3-C10 (0-7.189) C10-F4-C10 (0-8.087) C12-F1-C12 (0-4.942) C12-F6-C12 (0-6.290) C12-F7-C12 (0-7.189) C13-F5-F8-C13 (0-3.145-12.131) C13-F9-C13 (0-5.391)	[f]B15-C10-B15 (0- 8.006) B15-C12-B15 (0-6.079) B16-C13-B16 (0-5.782)
40%	C10: F1, F2, F3, F4, F5 (32.348, 10.675) C12: F6, F7 (13.478, 4.448) C13: F8, F9 (14.377, 4.744)	B15: C10, C12 (15.123) B16: C13 (4.744)
	C10-F1-C10 (0-4.942) C10-F2-C10 (0-8.986) C10-F3-C10 (0-7.189) C10-F4-F5-C10 (0-8.087-11.232) C12-F6-C12 (0-6.29) C12-F7-C12 (0-7.189) C13-F8-C13 (0-8.986) C13-F9-C13 (0-5.391)	B15-C10-B15 (0-10.675) B15-C12-B15 (0-4.448) B16-C13-B16 (0-4.744)

Note:
(a) "C10: F2, F3, F4" denotes that the facility placement at location C10, with F2, F3, and F4 assigned to it.
(b) "(24.261, 8.006)" indicates that the facility will receive 24.261 metric tons of WSF and produce 8.006 metric tons of pellets.
(c) "C10-F2-C10 (0-8.986)" means that the route begins from C10 with zero load, travels to F2, and ends the route back to C10 with a load of 8.986 metric tons of WSF.
(d) "B15: C10, C12" denotes that B15 are assigned with C10 and C12.
(e) "(14.085)" indicates that the biorefinery receives 14.085 metric tons of pellets.
(f) "B15-C10-B15 (0- 8.006)" indicates the truck starts from B15 without any load, transports 8.006 metric tons of pellets from C10, and returns to B15.

6   Conclusions

This research introduces a MINLP model for optimizing the Biomass Supply Chain (BSC) dedicated to converting palm oil biomass into biofuels. The model incorporates several crucial aspects:

1. **Simultaneous Decision Optimization**: It proposes an innovative approach to BSC decision-making by simultaneously optimizing locational, allocation, and routing decisions. This

comprehensive perspective ensures that all components of the supply chain work optimally together.

2. **Quantification of Pretreatment Operation**: Unlike previous models, this study quantifies the pretreatment operation and integrates it as an additional parameter within the model. This adds a layer of complexity and accuracy to the decision-making process.

3. **Multi-Objective Optimization**: The model addresses sustainability concerns from multiple dimensions, including economic, environmental, and social performance. It aims to minimize costs, reduce CO_2 emissions from transportation, and limit the total population affected by facility locations.

In conducting computational experiments, the study assessed how the model performs in both single and multi-objective optimization scenarios. Single-objective optimization revealed that the proposed objectives often contradict one another. While each objective optimizes well within its respective dimension, achieving one objective without negatively impacting others is challenging.

In multi-objective optimization, the weighted sum approach was employed to combine all objective functions. The findings showed trade-offs between the sustainability dimensions. Environmental performance was most affected, with a 43.9% increase in CO_2 emissions. Economic performance saw a negligible decline of 0.036%, and social performance decreased by 1.96%. Although multi-objective optimization may not yield results as favorable as optimizing each dimension individually, it provides decisions that balance trade-offs among all sustainable goals. The study emphasizes the significance of considering environmental and social impacts, as they profoundly affect human well-being.

The in-depth sensitivity parameter analysis demonstrates that transportation costs wield a substantial influence over both total expenses and CO_2 emissions in the supply chain. However, locational decisions remain unaffected by this parameter. With a total of 60.203 metric tons of WSF across all mills (F1 to F9), at least three collection facilities are necessary. Moreover, the model must strike a balance among the three objective functions. Therefore, C10, C12, and C13 are consistently recommended as the optimal locations for the test instance across all scenarios of percentage change. Although assignment, allocation, and routing decisions show some sensitivity to transportation costs, their flexibility is constrained by fixed facility locations, truck capacities, and demands. Consequently, their sensitivity to transportation costs is minimal.

Meanwhile, the CO_2 emission rates exert their impact solely on the total CO_2 emissions, with none of the decision variables exhibiting sensitivity to uncertainties in CO_2 emission rate parameters. These rates are linked to transportation distance and truck loads, often correlated with facility locations, truck capacity, and demands. Despite changes in CO_2 emission rates, decision-making remains constrained by factors such as facility locations and capacity, truck capacity, and demands, potentially explaining the lack of sensitivity in the model to CO_2 emission rates.

The varying capacities of collection facilities exert a noticeable influence on all objective functions, indicating the pivotal role this parameter plays in shaping various facets of the supply chain network. All decisions, encompassing locational, assignment, allocation, production, and routing decisions, demonstrate sensitivity to alternations in this parameter. Facility capacity directly affects the amount of WSF that can be collected, impacting decision variables within the constraints of truck capacity and demands. Reductions in facility capacity necessitate more facilities in the supply chain to collect WSF, resulting in expected adjustments in other decision variables. These findings highlight the model's sensitivity to the facility capacity parameter.

The research findings have several implications. Achieving all sustainable goals simultaneously can be challenging due to their inherent contradictions, necessitating trade-offs to be made. Adjustments in facility location and vehicle routing decisions are crucial to address these trade-offs effectively. Careful consideration should be given to factors such as truck conditions and fuel types due to their effects on transportation costs and CO_2 emission rates, which in turn influence total expenses and emissions within the supply chain. However, uncertainties in transportation costs have negligible impact on locational decisions and only limited effects on assignment, allocation, production, and routing decisions. Similarly, uncertainties in CO_2 emission rates do not affect decision variables in network configuration. Conversely, uncertainties in the capacity of collection facilities directly impact the achievement of all goals and decision variables, emphasizing their importance in supply chain management and necessitating meticulous attention.

The implications of the research are contingent upon the underlying assumptions of the model. The model is designed to address the location-routing problem under specific conditions, including the requirement that each mill be visited once and serve only one collection facility in the first echelon, and that each open collection facility be visited once and serve only one biorefinery. These assumptions limit the model's ability to handle scenarios where mills may require multiple visits or serve multiple facilities simultaneously in the first echelon, as well as analogous situations in the second echelon. Additionally, the model exclusively accounts for homogeneous trucks.

This research offers both practical and academic contributions. It provides a sustainable framework for industry professionals and policymakers to make strategic and operational decisions within the BSC. The framework assists in determining the number and locations of collection facilities and operational aspects like vehicle routing, biomass and pretreated biomass allocation, and pellet production. Moreover, the model is versatile and applicable to various facilities with different technologies, extending its utility beyond pelletizing technology.

From an academic perspective, the model can be applied to any BSC that optimizes facility locations, allocation, and vehicle routing decisions. It accommodates both single and multi-objective optimization, making it a valuable tool for addressing complex supply chain challenges. Furthermore, its integration of pretreatment operations differentiates it from standard 2ELRP models.

However, the proposed model assumes a homogeneous fleet of trucks, imposes restrictions on mill and collection facility visitation, and assigns equal importance to all objective functions during multi-objective optimization. These assumptions may not always align with real-world scenarios. Additionally, the model does not account for stochastic elements within the BSC. Future research can focus on addressing these limitations to enhance the model's applicability and accuracy.

Conflicts of Interest The authors declare no conflict of interest.

References

[1] M. Arabi, S. Yaghoubi & J. Tajik (2019). Algal biofuel supply chain network design with variable demand under alternative fuel price uncertainty: A case study. *Computers & Chemical Engineering*, *130*, Article ID: 106528. https://doi.org/10.1016/j.compchemeng.2019.106528.

[2] E. Asadi, F. Habibi, S. Nickel & H. Sahebi (2018). A bi-objective stochastic location-inventory-routing model for microalgae-based biofuel supply chain. *Applied Energy*, *228*, 2235–2261. https://doi.org/10.1016/j.apenergy.2018.07.067.

[3] N. Z. Atashbar, N. Labadie & C. Prins (2016). Modeling and optimization of biomass supply chains: A review and a critical look. *International Journal of Production Research*, *49*(12), 604–615. https://doi.org/10.1080/00207543.2017.1343506.

[4] J. X. Cao, X. Wang & J. Gao (2021). A two-echelon location-routing problem for biomass logistics systems. *Biosystems Engineering*, *202*, 106–118. https://doi.org/10.1016/j.biosystemseng.2020.12.007.

[5] J. X. Cao, Z. Zhang & Y. Zhou (2021). A location-routing problem for biomass supply chains. *Computers & Industrial Engineering*, *152*, Article ID: 107017. https://doi.org/10.1016/j.cie.2020.107017.

[6] L. E. Cárdenas-Barrón & R. A. Melo (2021). A fast and effective MIP-based heuristic for a selective and periodic inventory routing problem in reverse logistics. *Omega*, *103*, Article ID: 102394. https://doi.org/10.1016/j.omega.2021.102394.

[7] M. M. M. Chavez, Y. Costa & W. Sarache (2021). A three-objective stochastic location-inventory-routing model for agricultural waste-based biofuel supply chain. *Computers & Industrial Engineering*, *162*, Article ID: 107759. https://doi.org/10.1016/j.cie.2021.107759.

[8] N. H. Che Hamzah, A. Yahya, H. Che Man & A. Samsu Baharuddin (2018). Effect of pre-treatments on compost production from shredded oil palm empty fruit bunch with palm oil mill effluent anaerobic sludge and chicken manure. *BioResources*, *13*(3), 4998–5012. https://doi.org/10.15376/biores.13.3.4998-5012.

[9] A. De Meyer, D. Cattrysse & J. Van Orshoven (2015). A generic mathematical model to optimise strategic and tactical decisions in biomass-based supply chains (OPTIMASS). *European Journal of Operational Research*, *245*(1), 247–264. https://doi.org/10.1016/j.ejor.2015.02.045.

[10] J. E. Fokkema, M. J. Land, L. C. Coelho, H. Wortmann & G. B. Huitema (2020). A continuous-time supply-driven inventory-constrained routing problem. *Omega*, *92*, Article ID: 102151. https://doi.org/10.1016/j.omega.2019.102151.

[11] Greenhouse gas protocol. Calculation tools. Emission Factors from Cross-Sector Tools. https://ghgprotocol.org/calculation-tools 2017. Accessed: 2023-01-12.

[12] F. Habibi, E. Asadi & S. J. Sadjadi (2018). A location-inventory-routing optimization model for cost effective design of microalgae biofuel distribution system: A case study in Iran. *Energy strategy reviews*, *22*, 82–93. https://doi.org/10.1016/j.esr.2018.08.006.

[13] B. S. How & H. L. Lam (2017). Integrated biomass supply chain in Malaysia: A sustainable strategy. *Chemical Engineering Transactions*, *61*, 1573–1578. https://doi.org/10.3303/CET1761260.

[14] B. S. How, K. Y. Tan & H. L. Lam (2016). Transportation decision tool for optimisation of integrated biomass flow with vehicle capacity constraints. *Journal of Cleaner Production*, *136*(Part B), 197–223. https://doi.org/10.1016/j.jclepro.2016.05.142.

[15] L. Jayarathna, G. Kent, I. O'Hara & P. Hobson (2020). A Geographical Information System based framework to identify optimal location and size of biomass energy plants using single or multiple biomass types. *Applied energy*, *275*, Article ID: 115398. https://doi.org/10.1016/j.apenergy.2020.115398.

[16] KULIM. Integrated annual report: Unleashing potential strategic initiatives. Technical report KULIM Malaysia Berhad Johor, Malaysia 2019. https://kulim.com.my/storage/2023/06/KULIM-IAR-2019.pdf.

[17] K. Laasasenaho, A. Lensu, R. Lauhanen & J. Rintala (2019). GIS-data related route optimization, hierarchical clustering, location optimization, and kernel density methods are useful for promoting distributed bioenergy plant planning in rural areas. *Sustainable Energy Technologies and Assessments*, *32*, 47–57. https://doi.org/10.1016/j.seta.2019.01.006.

[18] H. L. Lam, W. P. Ng, R. T. Ng, E. H. Ng, M. K. A. Aziz & D. K. Ng (2013). Green strategy for sustainable waste-to-energy supply chain. *Energy*, *57*, 4–16. https://doi.org/10.1016/j.energy.2013.01.032.

[19] P. Lamers, M. S. Roni, J. S. Tumuluru, J. J. Jacobson, K. G. Cafferty, J. K. Hansen, K. Kenney, F. Teymouri & B. Bals (2015). Techno-economic analysis of decentralized biomass processing depots. *Bioresource technology*, *194*, 205–213. https://doi.org/10.1016/j.biortech.2015.07.009.

[20] E. León-Olivares, H. Minor-Popocatl, O. Aguilar-Mejía & D. Sánchez-Partida (2020). Optimization of the supply chain in the production of ethanol from agricultural biomass using mixed-integer linear programming (MILP): A case study. *Mathematical Problems in Engineering*, *2020*(1), Article ID: 6029507. https://doi.org/10.1155/2020/6029507.

[21] S. Li, Z. Wang, X. Wang, D. Zhang & Y. Liu (2019). Integrated optimization model of a biomass feedstock delivery problem with carbon emissions constraints and split loads. *Computers & Industrial Engineering*, *137*, Article ID: 106013.

[22] N. Mahjoub, H. Sahebi, M. Mazdeh & A. Teymouri (2020). Optimal design of the second and third generation biofuel supply network by a multi-objective model. *Journal of Cleaner Production*, *256*, Article ID: 120355. https://doi.org/10.1016/j.jclepro.2020.120355.

[23] K. T. Malladi, O. Quirion-Blais & T. Sowlati (2018). Development of a decision support tool for optimizing the short-term logistics of forest-based biomass. *Applied Energy*, *216*, 662–677. https://doi.org/10.1016/j.apenergy.2018.02.027.

[24] S. Mani, S. Sokhansanj, X. Bi & A. Turhollow (2006). Economics of producing fuel pellets from biomass. *Applied Engineering in Agriculture*, *22*(3), 421–426. https://doi:10.13031/2013.20447.

[25] M. A. Méndez-Vázquez, F. I. Gómez-Castro, J. M. Ponce-Ortega, A. H. Serafín-Muñoz, J. E. Santibañez-Aguilar & M. M. El-Halwagi (2017). Mathematical optimization of a supply chain for the production of fuel pellets from residual biomass. *Clean Technologies and Environmental Policy*, *19*, 721–734. https://doi.org/10.1007/s10098-016-1257-1.

[26] N. R. Menon, Z. Ab Rahman & N. A. Bakar (2003). Empty fruit bunches evaluation: Mulch in plantation vs. fuel for electricity generation. *Oil Palm Industry Economic Journal*, *3*(2), 15–20.

[27] F. Misni & L. S. Lee (2019). Harmony search for multi-depot vehicle routing problem. *Malaysian Journal of Mathematical Sciences*, *13*(3), 311–328.

[28] F. Misni & L. S. Lee (2021). Modified harmony search algorithm for location-inventory-routing problem in supply chain network design with product returns. *Malaysian Journal of Mathematical Sciences*, *15*(1), 1–20.

[29] Official Portal of Ministry of Finance Malaysia. Retail price of petroleum products from 8 December 2022 to 14 December 2022. Press Release. https://www.mof.gov.my/portal/en/news/press-release/retail-price/retail-price-of-petroleum-products-from-1-december-2022-to-7-december-2022 2022. Accessed: 2022-11-30.

[30] T. M. Pinho, J. P. Coelho, G. Veiga, A. P. Moreira & J. Boaventura-Cunha (2017). A multilayer model predictive control methodology applied to a biomass supply chain operational level. *Complexity*, *2017*(1), Article ID: 5402896. https://doi.org/10.1155/2017/5402896.

[31] A. Rahman, H. I. Tan, W. Liew & N. S. Shahruddin (2020). Routing mail delivery from a single depot with multiple delivery agents. *Malaysian Journal of Mathematical Sciences*, *14*(S), 15–29.

[32] S. Razm, A. Dolgui, R. Hammami, N. Brahimi, S. Nickel & H. Sahebi (2021). A two-phase sequential approach to design bioenergy supply chains under uncertainty and social concerns. *Computers & Chemical Engineering*, *145*, Article ID: 107131. https://doi.org/10.1016/j.compchemeng.2020.107131.

[33] L. Rivera-Cadavid, P. C. Manyoma-Velásquez & D. F. Manotas-Duque (2019). Supply chain optimization for energy cogeneration using sugarcane crop residues (SCR). *Sustainability*, *11*(23), Article ID: 6565. https://doi.org/10.3390/su11236565.

[34] M. S. Roni, S. D. Eksioglu, K. G. Cafferty & J. J. Jacobson (2017). A multi-objective, hub-and-spoke model to design and manage biofuel supply chains. *Annals of Operations Research*, *249*(1), 351–380. https://doi.org/10.1007/s10479-015-2102-3.

[35] M. Saadati & S. J. Hosseininezhad (2019). Designing a hub location model in a bagasse-based bioethanol supply chain network in Iran (case study: Iran sugar industry). *Biomass and Bioenergy*, *122*, 238–256. https://doi.org/10.1016/j.biombioe.2019.01.013.

[36] K. Sahoo, G. Hawkins, X. Yao, K. Samples & S. Mani (2016). GIS-based biomass assessment and supply logistics system for a sustainable biorefinery: A case study with cotton stalks in the Southeastern US. *Applied Energy*, *182*, 260–273. https://doi.org/10.1016/j.apenergy.2016.08.114.

[37] K. Sahoo, S. Mani, L. Das & P. Bettinger (2018). GIS-based assessment of sustainable crop residues for optimal siting of biogas plants. *Biomass and Bioenergy*, *110*, 63–74. https://doi.org/10.1016/j.biombioe.2018.01.006.

[38] S. F. Salleh, M. F. Gunawan, M. F. Zulkarnain & A. Halim (2019). Modelling and optimization of biomass supply chain for bioenergy production. *Journal of Environmental Treatment Techniques*, *7*(4), 689–695.

[39] J. L. G. San Juan, K. B. Aviso, R. R. Tan & C. L. Sy (2019). A multi-objective optimization model for the design of biomass co-firing networks integrating feedstock quality considerations. *Energies*, *12*(12), Article ID: 2252. https://doi.org/10.3390/en12122252.

[40] B. R. Sarker, B. Wu & K. P. Paudel (2018). Optimal number and location of storage hubs and biogas production reactors in farmlands with allocation of multiple feedstocks. *Applied Mathematical Modelling*, *55*, 447–465. https://doi.org/10.1016/j.apm.2017.11.010.

[41] B. R. Sarker, B. Wu & K. P. Paudel (2019). Modeling and optimization of a supply chain of renewable biomass and biogas: Processing plant location. *Applied Energy*, *239*, 343–355. https://doi.org/10.1016/j.apenergy.2019.01.216.

[42] T. Schröder, L.-P. Lauven & J. Geldermann (2018). Improving biorefinery planning: Integration of spatial data using exact optimization nested in an evolutionary strategy. *European Journal of Operational Research*, *264*(3), 1005–1019. https://doi.org/10.1016/j.ejor.2017.01.016.

[43] A. Serrano-Hernandez & J. Faulin (2019). Locating a biorefinery in northern Spain: Decision making and economic consequences. *Socio-Economic Planning Sciences*, *66*, 82–91. https://doi.org/10.1016/j.seps.2018.07.012.

[44] J. She, W. Chung & H. Han (2019). Economic and environmental optimization of the forest supply chain for timber and bioenergy production from beetle-killed forests in northern Colorado. *Forests*, *10*(8), Article ID: 689. https://doi.org/10.3390/f10080689.

[45] R. Soares, A. Marques, P. Amorim & J. Rasinmäki (2019). Multiple vehicle synchronisation in a full truck-load pickup and delivery problem: A case-study in the biomass supply chain. *European Journal of Operational Research*, *277*(1), 174–194. https://doi.org/10.1016/j.ejor.2019.02.025.

[46] T. Soha, L. Papp, C. Csontos & B. Munkácsy (2021). The importance of high crop residue demand on biogas plant site selection, scaling and feedstock allocation – A regional scale concept in a Hungarian study area. *Renewable and Sustainable Energy Reviews*, *141*, Article ID: 110822. https://doi.org/10.1016/j.rser.2021.110822.

[47] A. Sultana, A. Kumar & D. Harfield (2010). Development of agri-pellet production cost and optimum size. *Bioresource technology*, *101*(14), 5609–5621. https://doi.org/10.1016/j.biortech.2010.02.011.

[48] S. Tiammee & C. Likasiri (2020). Sustainability in corn production management: A multi-objective approach. *Journal of Cleaner Production*, *257*, Article ID: 120855. https://doi.org/10.1016/j.jclepro.2020.120855.

[49] E. B. Tirkolaee, P. Abbasian & G.-W. Weber (2021). Sustainable fuzzy multi-trip location-routing problem for medical waste management during the COVID-19 outbreak. *Science of the Total Environment*, *756*, Article ID: 143607. https://doi.org/10.1016/j.scitotenv.2020.143607.

[50] L. Torjai & F. Kruzslicz (2016). Mixed integer programming formulations for the biomass truck scheduling problem. *Central European Journal of Operations Research*, *24*, 731–745. https://doi.org/10.1007/s10100-015-0395-6.

[51] M. Vahdanjoo, M. Nørremark & C. G. Sørensen (2021). A system for optimizing the process of straw bale retrieval. *Sustainability*, *13*(14), Article ID: 7722. https://doi.org/10.3390/su13147722.

[52] R. Wang, S. Chang, X. Cui, J. Li, L. Ma, A. Kumar, Y. Nie & W. Cai (2021). Retrofitting coal-fired power plants with biomass co-firing and carbon capture and storage for net zero carbon emission: A plant-by-plant assessment framework. *GCB Bioenergy*, *13*(1), 143–160. https://doi.org/10.1111/gcbb.12756.

[53] H. Woo, M. Acuna, M. Moroni, M. S. Taskhiri & P. Turner (2018). Optimizing the location of biomass energy facilities by integrating multi-criteria analysis (MCA) and geographical information systems (GIS). *Forests*, *9*(10), Article ID: 585. https://doi.org/10.3390/f9100585.

[54] F. F. Yeng, Z. M. Zainuddin & H. S. Pheng (2024). Optimizing palm oil biomass supply chain logistics through multi-objective location-routing model. *Malaysian Journal of Fundamental and Applied Sciences*, 20(2), 247–265. https://doi.org/10.11113/mjfas.v20n2.3085.

[55] D. S. Zamar, B. Gopaluni & S. Sokhansanj (2017). Optimization of sawmill residues collection for bioenergy production. *Applied Energy*, 202, 487–495. https://doi.org/10.1016/j.apenergy.2017.05.156.

[56] F. Zhang, D. Johnson, M. Johnson, D. Watkins, R. Froese & J. Wang (2016). Decision support system integrating GIS with simulation and optimisation for a biofuel supply chain. *Renewable Energy*, 85, 740–748. https://doi.org/10.1016/j.renene.2015.07.041.

[57] F. Zhang, J. Wang, S. Liu, S. Zhang & J. W. Sutherland (2017). Integrating GIS with optimization method for a biofuel feedstock supply chain. *Biomass and Bioenergy*, 98, 194–205. https://doi.org/10.1016/j.biombioe.2017.01.004.

[58] X. G. Zhao & A. Li (2016). A multi-objective sustainable location model for biomass power plants: Case of China. *Energy*, 112, 1184–1193. https://doi.org/10.1016/j.energy.2016.07.011.